24th COBEM - 2017

24th ABCM International Congress of Mechanical Engineering
December 3-8, 2017, Curitiba, PR, Brazil

COBEM-2017-0644
CFD ANALYSIS OF A LOW SPEED SUBSONIC WIND TUNNEL

Olivio Ferreira Neto
Odenir de Almeida
Universidade Federal de Uberlândia, Faculdade de Engenharia Mecânica (FEMEC)
olivioneto@ufu.br; odenir.almeida@ufu.br

Abstract. *This work describes a flow analysis through Computational Fluid Dynamics (CFD) inside a low speed subsonic wind tunnel from CPAERO (Centro de Pesquisa em Aerodinâmica Experimental) at Federal University of Uberlandia. Full-scale model of the entire wind tunnel was considered and two configurations were tested: without corner-vanes (CV-out) and with corner-vanes (CV-in). The goal of this work was to analyze how the corner-vanes affected the flow inside the tunnel, especially at the test section. A finite volume formulation through Reynolds Averaged Navier-Stokes (RANS) method was applied to simulate the flow inside the tunnel. The standard k-ε and realizable k-ε models were employed for the turbulence modeling. After close analysis of the results, it was verified that the quality of the flow was significantly improved with the use of the corner-vanes, increasing the uniformity of the flow and making the streamlines more organized and uniform in the tunnel as a whole; however, at the test section the flow did not improve its uniformity, demanding a correction of the angle of the vanes positioned at the first corner. These simulations helped to develop the passive devices for flow control in the actual wind tunnel at CPAERO.*

Keywords: *wind tunnel, Aerodynamics, CFD, RANS, corner-vanes*

1. INTRODUCTION

Wind tunnels are significant research apparatus commonly used in aerodynamic investigations to study the effects of air moving past solid objects. To avoid the high expenditure of design and adaptation of this equipment, computational fluid dynamics (CFD) techniques are often used to precisely comprehend the flow profiles within the tunnel environment. These tools are used to help designing more efficient internal channels avoiding friction and pressure losses along the wind tunnel and, consequently, reducing the power to blow the air – Barlow et al. (1999).

A common design's objective for most wind tunnels is to obtain a flow in the test section that is parallel and steady flow with uniform speed throughout the test section. The fundamental principles used to model low-speed aerodynamic flows include mass conservation, force and motion relating to Newton's Second Law and energy exchanges governed by the First Law of Thermodynamics. In considering low-speed flows, the assumption of incompressible flow is often adopted to determine the correlation with respect to full-scale structural dynamic characteristics – Barlow et al. (1999). This procedure has been still applied in current wind tunnel designs; however, due to the availability of power computing and more accurate simulation procedures, viable numerical codes have been developed and applied to establish mathematical models involving flow and turbulence. Such numerical tools via CFD have become complementary and indispensable in a modern wind tunnel design.

Another relevant aspect is that apart from the overall flow profile, a precise evaluation of turbulence in wind tunnels is of paramount importance, while designing and commissioning the test-section. While simple mathematical models provide a global solution for the velocity profile, a well-developed CFD simulation may account for viscous and thermal boundary layers being developed throughout the various sections in the wind tunnel. Moreover, the impact of changing passive flow control devices could be evaluated in the simulations giving to the designer a broad range of opportunities to improve the equipment.

According to Chaudhry et al. (2015), the source of turbulence in wind tunnels can be briefly divided in two parts; turbulence due to eddies (vortex shedding, boundary layer, shear stress, and secondary flows) and noise (mechanical, vibration and aerodynamic). In this context, clearly the turbulence nature of the flow inside the wind tunnel could become very complex and affect the final measurements. This flow complexity would never be captured by using simple models and correlations, leaving to computational approaches the work of increasing the level of flow modeling.
In this work, a finite volume method through Reynolds-averaged Navier-Stokes solution (RANS) was applied to simulate the flow inside the tunnel. The main objective was to evaluate the flow quality in the test section. As turbulence modeling it were used standard k-ε and realizable k-ε models. Full-scale model of the entire wind tunnel was

considered instead of the conventional approach, in which only test section flow is simulated. This allowed for optimization of flow quality not only in the test section but also the flow in the entire circuit. Different wind tunnel configurations were tested: Without corner vanes (CV-out) and with corner vanes (CV-in).

Figure 1 describes a 3D representation of the wind tunnel of CPAERO of Federal University of Uberlandia, object of study in this work - Almeida et al. (2016).

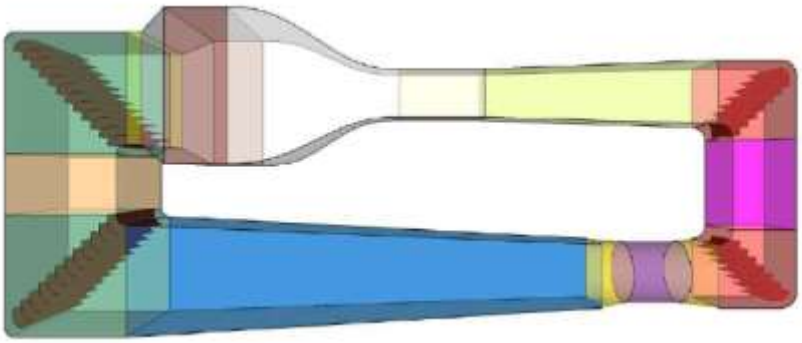

Figure 1. 3D representation of the wind tunnel (courtesy CPAERO, UFU).

2. WIND TUNNEL DESCRIPTION

The case study is a low-speed wind tunnel (subsonic at Mach 0.26) for research and educational purposes. It is a closed-circuit, closed-test-section with passive flow control through the use of corner-vanes and stabilization chamber. The main characteristics of this equipment are described below, according to Almeida et al. (2016):

- Closed-circuit and closed-test-section. Main width 10 m, length of approximately 30 m
- Naval-wood material applied for covering the side of sections.
- Metal rods used for the whole structure (skeleton) – fuselage type construction.
- The maximum air speed at test chamber around 90 m/s with a prescribed turbulence level of 0.2%.
- Minimum flow velocity: 5 m/s
- Test chamber dimensions: 1.7 m (spanwise) × 1.2 m (transversal) (area of 2.04m^2), with 3.0 m (length).
- Acrylic access doors.
- Stabilization chamber with screens and honeycombs for flow control.
- Contraction ratio of 12:1 in order to reach speed requirements.
- Drive System: Triphase 8 poles, 380 V and 350 hp equipped with an air cooling system, and fairing integrated in order to reduce flow disturbance and heating.
- Engine Speed control: through frequency inverter.
- Fan Blades: 8 blades of composite material, with approximately 3 m diameter and adjustable pitch for reaching optimal operational condition.
- The drive system is structural isolated from other sections of the tunnel, in order to avoid vibration to be transferred to the tunnel.

The Figure 2 shows a panoramic view of the constructed tunnel.

Figure 2. Panoramic view of the wind tunnel (Courtesy CPAERO, UFU).

3. NUMERICAL METHODOLOGY

The commercial ANSYS Fluent® numerical code was used for predicting the flow characteristics inside the closed-loop subsonic wind tunnel. As suggested by Moonen et al.(2006), a full-scale CFD model of the entire wind tunnel was considered instead of the conventional approach, in which only the flow in the test section was modeled. Thus, the entire model also accounted for the influence of the corner-vanes within the flow. This allowed for the optimization of the flow not only in the test section but also the flow in other wind tunnel sections. Moreover, the "conventional approach" was not suitable for designing new wind tunnels as it requires experimental data to simulate the test section inlet boundary conditions and was only useful for studying existing wind tunnel systems. Two sets of simulations were conducted: numerical 2D and 3D modeling of the wind tunnel without corner-vanes (CV-out) and numerical modeling of the wind tunnel with corner-vanes (CV-in).

The numerical code was used to solve the Reynolds averaged Navier–Stokes equation (RANS simulation) which employed a control-volume-based technique. The standard k-ε turbulence model was used for defining the turbulence kinetic energy and dissipation rate within the model, second-order upwind scheme was used to discretize all the transport equations. Standard wall functions were used on the walls and the roughness constant was set to 0.5. The numerical code used the semi-implicit method for pressure-linked equations (SIMPLE) algorithm for the velocity–pressure coupling of the computation. The rationale behind choosing the k-epsilon model was based on the findings of previous work from Calautit et al. (2014), which showed its capabilities in predicting the wind tunnel flows.

3.1 Computational Mesh

The mesh generation combined the advantages of a "*structured*" with those of an unstructured grid to minimize the computational cost. Sections of the wind tunnel that were of simple geometry in which one-dimensional flow dominates were meshed with quad-mesh. In the sections of complex geometry with three-dimensional flow such as the contraction and in the areas of the guiding vanes, quad/triangle cells were used.

The orthogonally and skewness were the parameters used to achieve the best quality of the mesh possible without making it too expensive in grid points. Different types of meshes were tested for the 3D models and the ones with the best characteristics cited were chosen for the final simulations, presented in this work. The mesh used to model the tunnel without the corner vanes had approximately 1,876,424 elements. Fig. 3 shows the cited mesh, including details in a zoom-view of the contraction and test section areas.

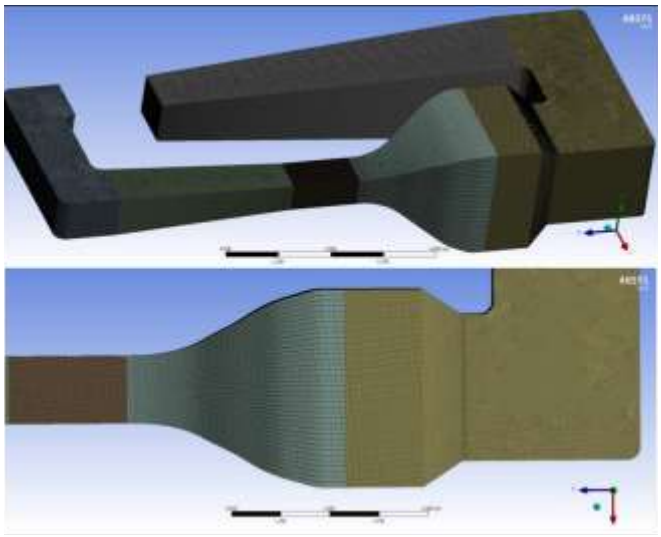

Figure 3. Details of the mesh – wind tunnel without corner-vanes (CV-out).

3.2 Boundary Conditions

The analytical model for estimating the pressure losses was directed as "intake fan" boundary conditions of the CFD model. A uniform boundary condition of the desired velocity was imposed along the inlet surface (intake fan) and the outlet (pressure outlet) was set to zero-gauge pressure. Air temperature of 25°C (298.15 K) was applied as inlet boundary condition to the flow and the velocity-inlet set as indicated in Fig. 4 by the white-arrow. The maximum velocity that the drive-system will impose on the flow is still unknown in practice, but it is expected with the tunnel unsealed, that it will be between 30 and 35 m/s. Based on that, it was chosen the inlet velocity for the simulations of 35 m/s. In this way, it was possible to observe how the corner vanes would modify the flow near the maximum velocity of the tunnel.

The screens and the honeycombs used in the actual CPAERO tunnel were not represented in the numerical model, as a simplification, due its complexity to represent and to maintain the computational costs not too high. This simplification implied some problems and will be discussed on the section of results.

The wind tunnel with the corner vanes demanded an expensive mesh, since the vanes had complex geometry, therefore the mesh used to model the tunnel had 16,190,530 elements and followed the cited method before. The whole mesh had approximately 91% of its elements as quadrilateral (quads). The Fig. 4 shows the mesh of the tunnel with the corner-vanes, as well as a zoom view of the refinement at the first corner.

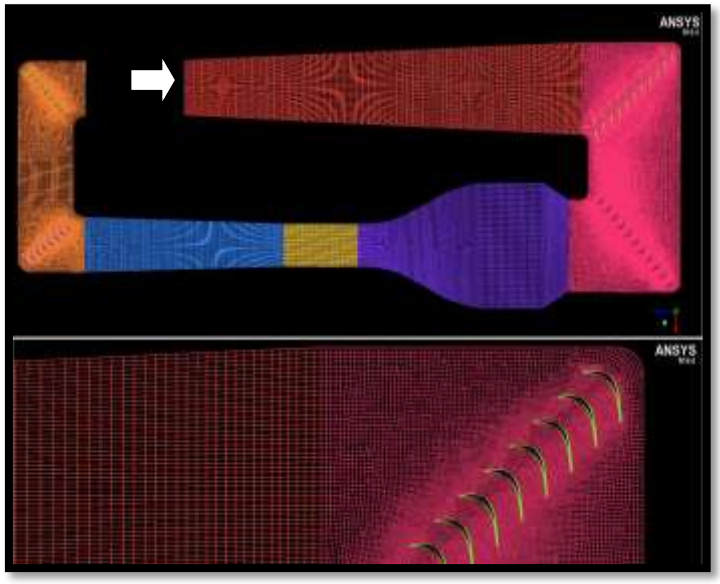

Figure 4. Mesh of the tunnel with corner-vanes (CV-in) at first corner.

4. RESULTS AND DISCUSSION

Based on the numerical setup described herein, the turbulent flow-fields were determined for the respective wind tunnel configurations. As results of these simulations, the velocity contours, the path lines and the velocity profiles will be presented and discussed. Velocity contours and path lines were used as a qualitative data to assess the flow characteristics along the wind tunnel sections, while the velocity profiles were used to evaluate the flow uniformity. Therefore, the main observations from the simulations were related to:

• Comparison of the flow quality (uniformity) in the test section adding the corner-vanes to the tunnel;

• Observation of the difference in the velocity profiles and magnitude of velocity in the test section adding the corner-vanes to the tunnel;

• Evaluation of the flow pattern at each section.

4.1 Velocity Contours

The velocity contours results for the flow inside the wind tunnel without corner-vanes (CV-out) and with corner-vanes installed on (CV-in) are seen in Figures 5 and 6, respectively. In Fig. 5 it was possible to analyze how much the flow was being accelerated and its general behavior at each section of the wind tunnel. The settling chamber placed before the contraction on the wind tunnel was effective to provide good flow uniformity at the test section and the designed contraction was able to accelerate the flow from 35 m/s at inlet to approximately 70.556 m/s (averaged) at the test section, an increase factor of approximately 2.016. However, it is also possible to observe flow separations in the upstream and downstream side of the wind tunnel corners. Moreover, due to the fact that screens and honeycombs were not represented in the model, it was possible to see how the flow was affected in that location. Despite the fact that the contraction itself helped to align the flow inside the test-section, clearly inside the settling chamber the flow is not well organized which impose losses to the main flow. A detailed analysis of the flow quality at the test section will be made by inspecting the velocity profiles in the test section.

With the inclusion of the corner-vanes (Fig. 7), the flow at the test section was surprisingly not better organized and more uniform than the case (CV-out). In this situation, the flow simulation helped to identify an important aspect related to the positioning of the corner-vanes. The cause of this problem was due to the vanes positioned at the first corner (coming from the inlet), that were not completely turning the flow by 90 degrees. Figures 7 and 8 below, illustrates the positioning of the corner-vanes and the flow pattern at those locations.

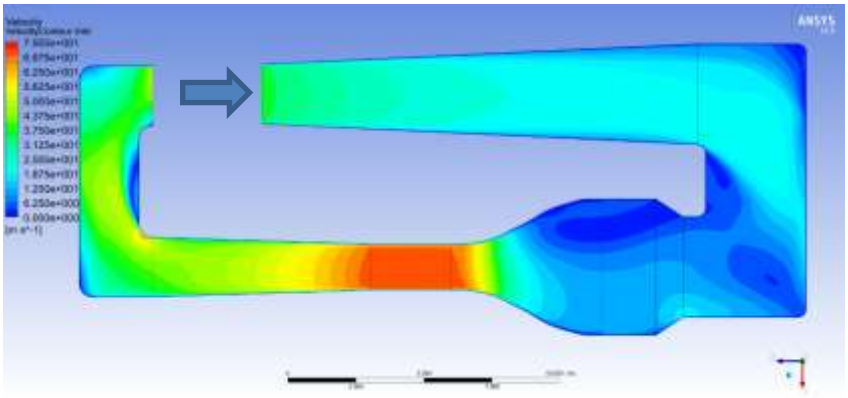

Figure 5. Velocity contour inside the tunnel without corner-vanes (CV-out).

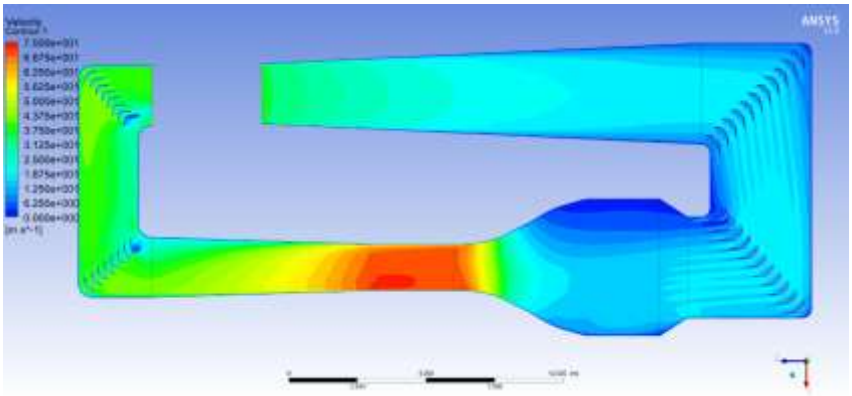

Figure 6. Velocity contours inside the tunnel with corner-vanes (CV-in).

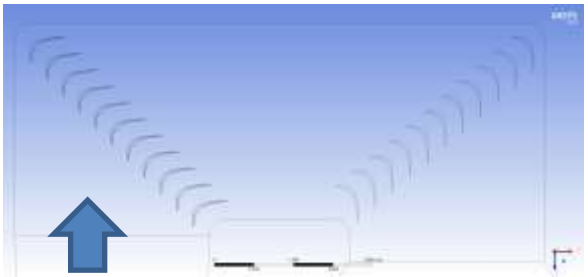

Figure 7. Details of the corner-vanes positioning.

Figure 8. Surface streamlines at the first corner.

After the analysis, it was concluded that the upstream vanes must be pivoted by 5 degrees in order to completely turn the flow at the bend (90º). This has been also identified in the work of Lindgren and Johansson (2002). Due to the high computational cost associated to the 3D simulation with corner vanes, it was not possible to accomplish such task since there were not enough time to make this correction and to analyze the results for this configuration, pointing the similarities and differences to the work of Calautit et al. (2014). Nevertheless, it is important to emphasize that the CPAERO wind tunnel has a passive control for angle in each corner-vane. It has two axis that allow to turn them, this way if any correction is needed, it is easy to implement it in the real configuration.

4.2 Pathlines

Path lines for the flow inside the wind tunnel are presented in Figures 9, 10, 11 and 12. Through these plots it is possible to see how the flow was well organized and with less vortices and swirls with the addition of the guide-vanes. However in the test section the flow was dislocated to the left from the natural direction it should follow, as it is shown on the Fig 11. The swirls that the flow is developing right after the second turn are due to the abrupt increase of the tunnel area imposed by the transition from the corner to the settling chamber, which detaches the flow at that location. It is important to point out that the honeycombs and the screens, not represented on the simulation, would increase the uniformity of the flow (screens), remove its swirls (honeycomb) and the flow would probably not detach as it is happening according to the simulation. Clearly, these devices for controlling the flow at the settling chamber (screens and honeycombs) are quite difficult to simulate due to geometric restrictions and size of them.

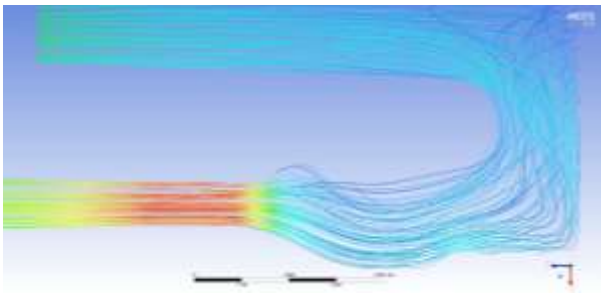

Figure 9. Path lines inside the tunnel without corner-vanes (superior view).

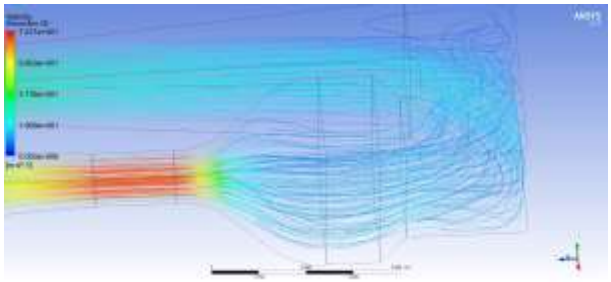

Figure 10. Path lines inside the tunnel without corner-vanes (perspective view).

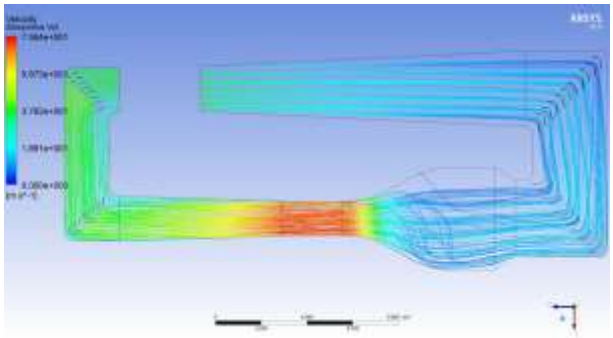

Figure 11. Path lines inside the tunnel with the corner-vanes (superior view).

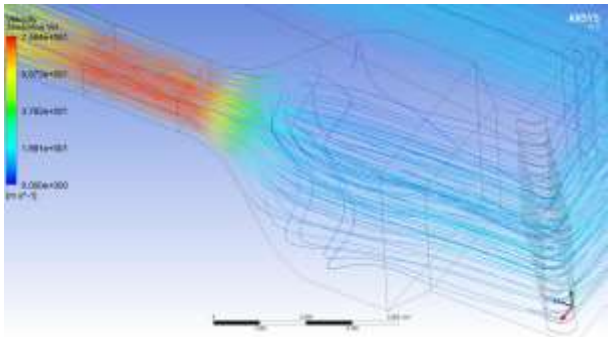

Figure 12. Path lines inside the tunnel with the corner-vanes (second view).

4.3 Velocity Profiles

The velocity profiles at different wind tunnel locations for both configurations (CV-in) and (CV-out) are presented in the following sub-sections. The height-velocity (Y) profile and width-velocity profiles (Z) were chosen, as seen in Fig. 13, in order to have a better understanding of the flow quality at each section. Despite the fact that the most important part is the test-section; it is interesting to understand the flow in other sections, which could help to improve the flow at each one by means of the passive flow control devices such as the turning-vanes, for example. By applying this procedure at some specific part of the wind tunnel the flow quality at the test section could be improved as well. The positions where the velocity profiles were obtained are shown on Fig. 13, each line (Y) and (Z) is one profile taken.

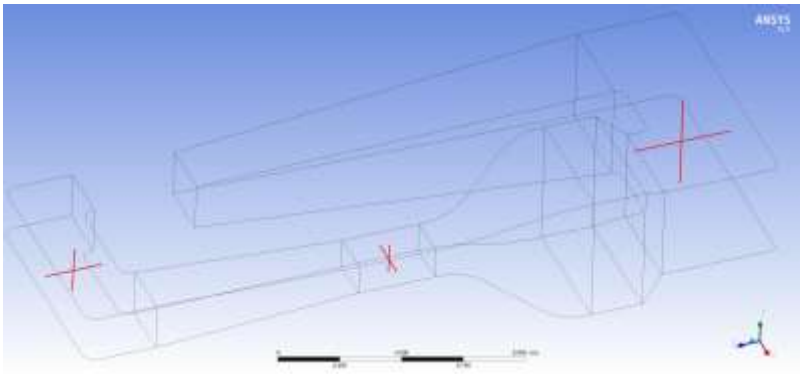

Figure 13. Positions where the velocity profiles were extracted.

The Y-axis was adopted as the height of the section being analyzed and the velocity at that location was normalized by the perpendicular component namely U_{max}, thus U/U_{max}. Therefore, U_{max} was the maximum velocity of the flow at that section, for each tunnel configuration, and U is the calculated local velocity at each point. These velocities profiles are shown in the next sub-section according to its specific location.

4.4 Test section-Profiles

The velocity profiles obtained from the 3D simulations of the wind tunnel with and without corner-vanes are shown on Figure 14. The flow the presence of the without the corner-vanes had a standard deviation of 1.22%, as the flow with the corner-vanes had a value of 1.70%. Comparing the mean velocities (width profile) of the two tunnel configurations, the difference was only 0.22%. It is possible to observe that the corner vanes made a very small difference on the flow quality at the test section, despite that, its influence was not good, making the reference case better than with the vanes installed. It is important to analyze this result by considering what was discussed about the influence of the corner-vanes angles, as pointed before. The benefit of the corner-vanes could be improved in this configuration by changing its angle of attack and improving the flow at the corner as well as in the contraction section. By doing this, it is expected that the flow inside the test-section could improve as well. This result has been a very important contribution of this work, which allowed a more detailed analysis of the flow within the wind tunnel channels.

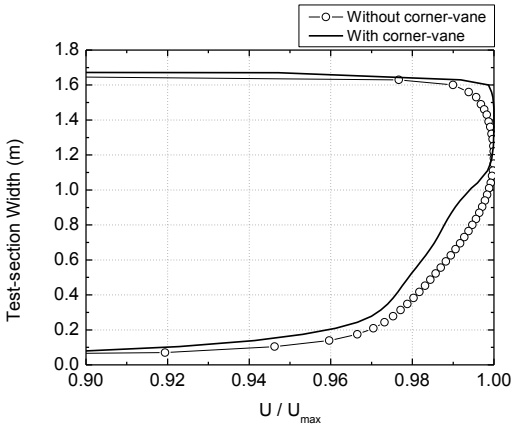

Figure 14. Velocity profile of the flow at the test section (width).

The next profile (Fig. 15) is the height profile at test section (y direction).

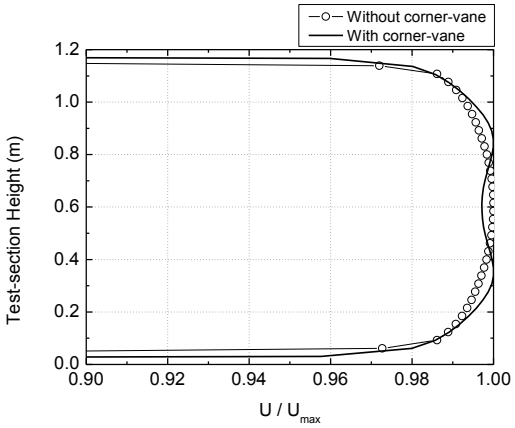

Figure 15. Velocity profile of the flow at the test section (height).

Analyzing the profile, Fig. 15, it is hard to point out if the flow improved its quality on the y direction (height) with the vanes installation, since the standard deviation for both tunnel configurations were 0.4% and the difference of the mean velocities of each configuration was 0.28%.

4.5 Bigger corner (Upwind corner)

The bigger corner is that one after the long diffuser or upstream of the test-section, as seen in Fig.1. Figure 16 shows the width-velocity profile of the flow.

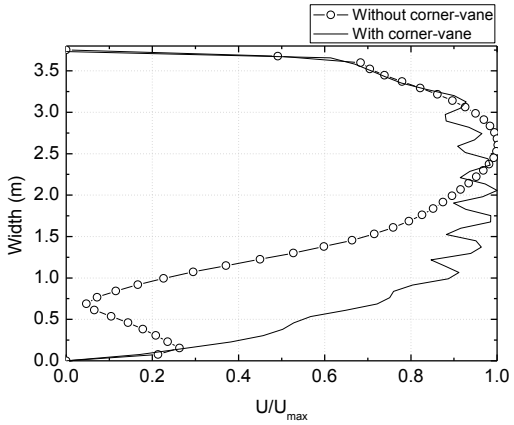

Figure 16. Velocity profile of the flow at upwind corner (width).

At the upwind corner the flow improved its quality in the z direction (width) with the placement of the vanes, the standard deviation improved from 42.65% to 16.91%. The lobes in the figure are due the presence of the corner-vane.

The next profile (Fig. 17) was taken in height (Y) at the same location in that section.

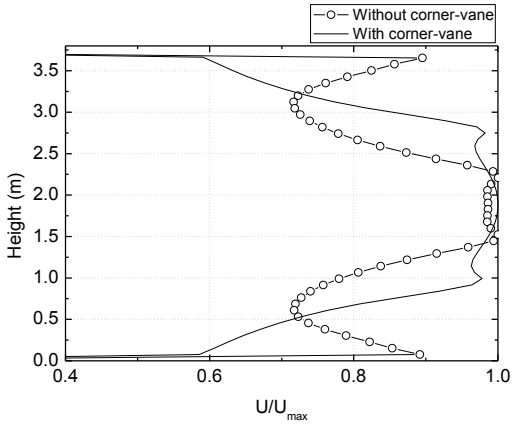

Figure 17. Velocity profile of the flow at upwind corner (height).

The transversal profile of the velocity at the upwind corner was improved with the inclusion of the corner-vanes. The standard deviation improved by 1%, but the profile showed a better organization of the flow than the reference case (without corner-vane).

4.6 Smaller corner (Downwind corner)

The flow quality at the downwind corner is the one that less influences the flow at test section, since as soon as it leaves the cited section it enters the pumping chamber, where it will gain high amount of energy and turbulence. Nevertheless, the flow quality at this section will be analyzed too. The profile shown on Fig.18 is the width-velocity profile.

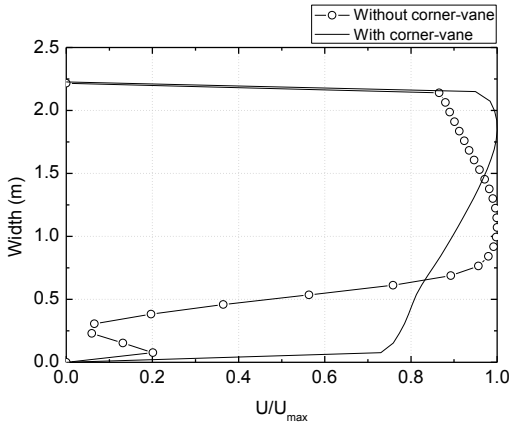

Figure 18. Velocity profile of the flow at downwind corner (width).

Visibly, the flow was well organized after the insertion of the vanes. While the standard deviation of the reference case flow was 31.9%, this value was 8.38% for the configuration with the vanes, showing a great improvement in its uniformity.

The last velocity profile to be shown is the one for the height, at the same section (downwind corner), Fig. 19.

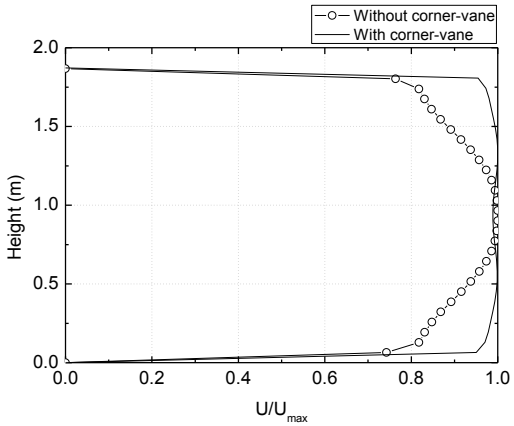

Figure 19. Velocity profile of the flow at downwind corner (height).

Following the same behavior of the width profile, the flow was well organized and a great quality was seen after the corner-vanes.

5. CONCLUSIONS

A numerical investigation of the flow parameters in a closed-loop subsonic wind tunnel was carried out by means of Computational Fluid Dynamics (CFD). A uniform boundary condition of the design-velocity was imposed along the inlet surface (intake fan) and a pressure outlet was set to zero-gauge. No porous-media was applied to emulate the honeycombs and screens. A full-scale CFD model of the wind tunnel was considered instead of the conventional approach. This allowed for the optimization of the flow quality not only in the test section but also the overall flow in other wind tunnel sections.

The difficulties of the work were mainly due to the size of the tunnel, which demanded a high number of cells to mesh, especially in the representation of the complex geometry of the corner-vanes. Adding the corner-vanes to the

tunnel improved the uniformity of the flow, however at the test section some distortions were observed mainly due to an incorrect angle of the vanes positioned in the first corner. These limitations affected the simulations which were time consuming and some of the corrections for the problem were not a viable option for presenting in this work. These corrections are currently being performed and a complementary study will analyze the flow with the new configuration and presented later.

The value of the data is its use in improving the comparisons between the results of other numerical models by providing a common benchmark. Furthermore, the data can be used for training of CFD users and contribute to an overall improvement of the prediction accuracy of CFD modeling of wind tunnels. Also, the data can be used to explore different optimization of the full closed-loop wind tunnel design and its separate components. The study evaluated the influence of the presence of guide vanes on the test section's flow quality (uniformity of the velocity flow field). Detailed investigation of the performance of the guide-vane such as shape, chord length and curvature was outside the scope of the study.

6. ACKNOWLEDGEMENTS

The authors would like to thank the FINEP (0138/11) for funding the wind tunnel design and the administration of Federal University of Uberlândia (UFU) for all support during the phases of this project. Also, the authors recognize the support from Fundação de Amparo a Pesquisa do Estado de Minas Gerais – FAPEMIG.

7. REFERENCES

Barlow, J., Rae, W., Pope, A., 1999. A., *Low-Speed Wind Tunnel Testing*, John Wiley & Sons, Third Edition.

Chaudhry, H.N., Calautit, J.K., Hughes, B.R., Sim, L.F., 2015. "CFD and Experimental Study on the Effect of Progressive Heating on Fluid Flow inside a Thermal Wind Tunnel". Computation, 3, 509-527.

Almeida, O., Miranda, F.C., Neto, O.F., Saad, F.G., 2016. "Design and Construction of a Low Speed Wind Tunnel". In Proceedings of 16th Brazilian Congress of Thermal Sciences and Engineering, Vitória, ES, Brazil.

Moonen, P., Blocken, B., Roels, S., Carmeliet, J. 2006. "Numerical modeling of the flow conditions in a closed-circuit low-speed wind tunnel". J. Wind Eng. Ind. Aerodyn. 94, 699–723.

Calautit, J.K., Chaudhry, H.N., Hughes, B.R., Sim, L.F., 2014. "A validated design methodology for a closed-loop subsonic wind tunnel". J. Wind Eng. Ind. Aerodyn. 125, 180–194.

Lindgren, B., Johansson, A.V., 2002. "Design and Evaluation of a Low-Speed Wind-Tunnel with Expanding Corners". Technical Report, Royal Institute of Technology, Sweden, 47p.

8. RESPONSIBILITY NOTICE

The authors are the only responsible for the printed material included in this paper.